

Particle Asymmetries from Quantum Statistics

Nikita Blinov

SLAC National Accelerator Laboratory, 2575 Sand Hill Road, Menlo Park, CA, 94025, USA

Anson Hook

Stanford Institute for Theoretical Physics, Stanford University, Stanford, CA 94305, USA

(Dated: May 23, 2017)

We consider a class of baryogenesis models where the Lagrangian in the visible sector is Charge-Parity (CP) invariant and a baryon asymmetry is produced only when quantum statistics is taken into account. The CP symmetry is broken by matter effects, namely the assumption that the primordial plasma contains another asymmetric species, such as dark matter. Out-of-equilibrium baryon number violating decays can then generate an asymmetry through Bose enhancement and/or Pauli blocking of certain decay channels.

I. INTRODUCTION

The origin of the observed excess of matter over anti-matter in the universe is one of the fundamental questions in particle physics [1]. A dynamical explanation must satisfy Sakharov's three criteria: violation of baryon number (B), violation of charge (C) and charge-parity (CP) invariance, and a departure from thermal equilibrium [2]. In many proposed scenarios CP violation is intrinsically tied to the departure from thermal equilibrium. For example, in electroweak baryogenesis CP -violating interactions with the advancing bubble wall (which drives plasma just outside out of equilibrium) are responsible for the generation of a chiral asymmetry that is then reprocessed into baryons [3, 4]. In the standard out-of-equilibrium decay scenarios like GUT baryogenesis and leptogenesis, the couplings of the decaying particle violate CP , allowing for an asymmetry to be created (see Refs. [5, 6] and the reviews [7–9]). In this paper, we explore a class of models where CP violation and the departure from thermal equilibrium are disentangled. We consider scenarios where an existing asymmetric particle density biases an otherwise CP -conserving process through the effects of quantum statistics, i.e. Pauli blocking and Bose enhancement, resulting in baryon number production.

Charge-Parity violation can occur in ways that are not seen in the visible sector Lagrangian. After all, the prevalence of baryons over anti-baryons is itself a violation of CP . Thus, it is clear that aside from a fundamental parameter in the Lagrangian, CP can also be violated by matter effects, i.e. by any pre-existing charge densities. This matter-induced CP violation has the distinct advantage of typically being testable if the charge corresponding to the asymmetry is conserved until late times. For example, this is the case for asymmetric dark matter (DM). The asymmetry and stability on cosmological time scales guarantee that there is a particle currently present in the universe that has a CP -violating number abundance. Note that we make a distinction between the CP breaking number abundances and the CP breaking Lagrangian parameters that they often come from (for some exceptions see Ref. [10–13]). We will consider the case where physics in the visible sector is CP -preserving (up to the Standard Model (SM) Cabibbo-Kobayashi-Maskawa phase) and CP violation in the early universe results from the presence of an asymmetric particle population rather than CP violation that might have caused their production.

There are several observed particles that can break CP with their number densities and therefore can be used to implement baryogenesis. Photons and gravitons can be chiral and thus break CP . For example, chiral magnetic fields in the early universe can generate a $B + L$ asymmetry via the weak anomaly [14–17], while chiral gravitational waves can source a $B - L$ asymmetry through the gravitational anomaly [18].

A dark matter asymmetry can also source the creation of baryon number. There are many ways to achieve this. The asymmetric dark matter (ADM) paradigm postulates that dark matter *carries* baryon number. Thus an asymmetry in DM entails an asymmetry in baryons; it is communicated to the SM via a transfer operator [19]. However, in this case, dark matter is not the source of CP violation, but rather a hidden reservoir of baryons (or anti-baryons [20]). The alternative we consider in this work utilizes the fact that the DM number density $J_D^0 \neq 0$ breaks CP , which can be used to generate baryon number from an otherwise CP preserving decay. The existence of a chemical potential splits the energy levels of particles and anti-particles. As a result, the CPT symmetry is broken in this non-vacuum background. This can also be seen from the fact that J_D^0 is CPT odd and non-zero in the presence of a dark asymmetry. Thus, CPT breaking allows for baryon asymmetry production at tree level without any interference effects. The use of a CPT -violating background is similar in spirit to models of spontaneous baryogenesis [21, 22]¹. Another example of this effect is the use of J_D^0 to generate a CP violating coupling in the Lagrangian much in the same way that the Higgs vacuum expectation value allows for one to write a $SU(2)_W$ breaking Lagrangian coupling [23].

In this paper, we use quantum statistics to transmit the CP violation from the dark sector to the SM. As a simple example of this mechanism in action, consider the out-of-equilibrium decays of a real scalar φ with the interaction

$$\mathcal{L} \supset \frac{1}{\Lambda} \varphi \psi_B \psi_D \phi_D^\dagger + \text{h.c.} \quad (1)$$

where ψ_B is a fermion that carries baryon number and ψ_D (ϕ_D) is a fermion (scalar) that carries a $U(1)_D$ dark quantum number. This interaction gives rise to two decay channels for φ ,

$$\varphi \rightarrow \psi_B \psi_D \phi_D^\dagger \quad (2)$$

$$\varphi \rightarrow \psi_B^\dagger \psi_D^\dagger \phi_D. \quad (3)$$

The decays of φ violate baryon number but preserve dark matter number. In the absence of any CP violation, Lagrangian or otherwise, these two decays have equal probabilities so that no baryon number asymmetry is generated.

¹ In the model given in Eq. 1, one can explicitly see the difference between spontaneous baryogenesis and the models we consider in this paper. If the interactions were in thermal equilibrium, then there would be no baryon number generated.

Now suppose that the existing DM density is asymmetric: the plasma contains more ψ_D^\dagger (ϕ_D^\dagger) than ψ_D (ϕ_D). Given the simple set-up above, this is the only source of CP violation. At finite density and temperature, the φ decay rate includes the effects of Pauli blocking and Bose enhancement due to the existence of the final state particles in the plasma. As a result the channel 2 is preferred over 3, so the decays produce a baryon number asymmetry. In the limit of a large dark matter asymmetry, the anti-baryon channel 3 can be completely forbidden. We see that both boson and fermion statistics generate an asymmetry with the same sign at tree level. As we will show in Sec. II, the effect of Bose enhancement is significantly larger than Pauli exclusion for this model.

In the scenarios we consider the baryon asymmetry is roughly bounded from above by the dark sector asymmetry. If this asymmetry persists to late times, the dark sector particle must be lighter than baryons since $\Omega_{\text{cdm}}/\Omega_b \sim 5$. However, if these states eventually decay, their mass is not constrained. In what follows, we refer to the asymmetric dark sector states as DM, even if they are unstable on cosmological timescales and do not comprise the entire DM density of the universe today.

Standard baryogenesis via out-of-equilibrium decay is an “infra-red dominated” process, in which the decays of the particle and the desired asymmetry are generated at the same time $t \sim H^{-1} \sim \Gamma_\varphi^{-1}$, where Γ_φ is the φ decay rate. The small fraction of decays that occur when $\Gamma_\varphi t \ll 1$ is irrelevant for the production of the asymmetry. This intuition rests on the assumption that the decay asymmetry does not depend on temperature. In contrast, in the models where quantum statistics is responsible for the generation of the asymmetry, we find important temperature dependence. As we describe in the following sections, this causes the majority of the asymmetry to be produced at early times, well before $t \sim \Gamma_\varphi^{-1}$.

This paper is organized as follows. In Section II, we consider the model of Eq. 1 in detail. We show numerically and analytically that Bose enhancement of individual decay channels can result in a baryon asymmetry parametrically of the same size as the dark matter asymmetry. Surprisingly, we find that for certain parameters the baryon asymmetry can be larger by $\mathcal{O}(1)$ factors. In Section III, we present a second model where Pauli exclusion rather than Bose enhancement is the dominant effect responsible for generating a large asymmetry in the visible sector. We discuss our results and conclude in Section IV.

II. ASYMMETRIES THROUGH BOSE ENHANCEMENT

In this section, we examine the model presented in the introduction. We consider the Lagrangian

$$\mathcal{L} \supset \left(\frac{1}{\Lambda} \varphi \psi_B \psi_D \phi_D^\dagger - m_{\psi_D} \psi_D \psi_D^c - m_{\psi_B} \psi_B \psi_B^c + \text{h.c.} \right) - m_{\phi_D}^2 |\phi_D|^2. \quad (4)$$

The fermion ψ_B carries baryon number B and its interactions with φ break B . We assume that an asymmetry in ψ_B can be converted into a SM baryon asymmetry through, e.g., the neutron portal

$$\mathcal{L} \supset \frac{1}{\Lambda^2} \psi_B u_R^c d_R^c d_R^c + \text{h.c.} \quad (5)$$

We neglected the allowed interaction $\varphi \psi_B \psi_D^c \phi_D / \Lambda'$. If included, it would not qualitatively change the results as long as $\Lambda' \neq \Lambda$.

Chemical equilibrium among the dark sector states ψ_D and ϕ_D can be maintained with the inclusion of additional states that can mediate the reaction $\psi_D \psi_D \leftrightarrow \phi_D \phi_D$. This process can occur through an s -channel exchange of a $U(1)_D$ -charged scalar Φ with interactions

$$\Phi^\dagger \phi_D \phi_D + \Phi^\dagger \psi_D \psi_D + \Phi \psi_D^c \psi_D^c + \text{h.c.}, \quad (6)$$

or through a t -channel fermion mediator χ coupling to DM via

$$\phi_D^\dagger \psi_D \chi + \phi_D \psi_D^c \chi + \text{h.c.} \quad (7)$$

In what follows we remain agnostic to the origin of the chemical equilibration of DM with itself. The first term in Eq. 4 combined with one of the equilibration mechanisms above generates a Majorana mass for ψ_B , which is small for parameters of interest (where φ decays out of equilibrium) and will be ignored.

We imagine that the scalar φ decays far out of equilibrium when the universe is already populated by asymmetric dark matter. At finite temperature the rate for a single decay channel is

$$\Gamma(\varphi \rightarrow \psi_B \psi_D \varphi_D^\dagger) = \frac{1}{2M_\varphi} \int d\Phi_3 |\mathcal{M}|^2 (1 + f_{\phi_D})(1 - f_{\psi_D})(1 - f_{\psi_B}), \quad (8)$$

where \mathcal{M} is the decay matrix element, $d\Phi_3$ is the three-body phase space volume element. The distribution functions f_i have their equilibrium Bose-Einstein or Fermi-Dirac forms

$$f_{\text{BE,FD}} = \left[\exp \left(\frac{E - \mu}{T} \right) \mp 1 \right]^{-1}, \quad (9)$$

for bosons and fermions, respectively. The sign of the chemical potentials is reversed for anti-particle distributions. Chemical potentials are related to particle density asymmetries via

$$\Delta n_i = n_i - n_{\bar{i}} = g_i \int \frac{d^3p}{(2\pi)^3} [f(E, \mu) - f(E, -\mu)], \quad (10)$$

where g_i is the number of internal degrees of freedom of species i . We require that $|\mu_{\phi_D}| < m_{\phi_D}$ in order to avoid ϕ_D getting a vacuum expectation value.

The product of statistical factors in Eq. 8 encodes stimulated emission (Bose enhancement) and Pauli blocking by the particles already present in the bath. Note that their effects are large in the region of phase space where the final state particles are produced with energy less than T . As we will be taking $M_\varphi \gg T$, when one particle has energy $\lesssim T$, the other two will have large energies of order M_φ .

The total width of φ at leading order in T/M_φ is given by

$$\Gamma_\varphi = \Gamma(\varphi \rightarrow \psi_B \psi_D \phi_D^\dagger) + \Gamma(\varphi \rightarrow \bar{\psi}_B \bar{\psi}_D \phi_D) = \frac{1}{768\pi^3} \frac{M_\varphi^3}{\Lambda^2}. \quad (11)$$

The dependence on chemical potentials of final state particles and the effects of the statistical factors enter at higher order in T/M_φ . In the right panel of Fig. 1, we show the numerical and analytic results for the total width. As long as $M_\varphi \gtrsim 3T$, the analytic estimate provides a good approximation for the total width. The decay width determines the number density of φ through the Boltzmann equation

$$\dot{n}_\varphi + 3Hn_\varphi = -\Gamma_\varphi n_\varphi. \quad (12)$$

The out-of-equilibrium assumption ensures that inverse decays are not important.

As φ decays, an asymmetry $\Delta n_{\psi_B} \neq 0$ can be generated because the rates for the two decay channels of φ are not equal when the DM is asymmetric, i.e. when there are non-zero chemical potentials for ϕ_D and ψ_D . The resulting production of baryon number is governed by

$$\Delta \dot{n}_{\psi_B} + 3H\Delta n_{\psi_B} = \Delta \Gamma n_\varphi, \quad (13)$$

where the decay asymmetry

$$\Delta \Gamma = \Gamma(\varphi \rightarrow \psi_B \psi_D \phi_D^\dagger) - \Gamma(\varphi \rightarrow \bar{\psi}_B \bar{\psi}_D \phi_D) \quad (14)$$

depends implicitly on the abundances of ψ_D , ϕ_D and ψ_B through their chemical potentials - see Eq. 10. Since the observed baryon asymmetry $n_{\psi_B}/s \sim 10^{-10}$, we can restrict our attention to small chemical potentials $\mu/T \ll 1$, such that $\Delta \Gamma$ is linear in Δn_i to a good approximation. An analytic expression for $\Delta \Gamma$ can be obtained in the interesting limit $\mu/T \ll m_{\phi_D}/T \ll T/M_\varphi \ll 1$ ²

$$\Delta \Gamma = \Gamma_\varphi \left[12 \ln \left[\frac{m_{\phi_D}^2}{2T^2} \right] \frac{\mu_{\phi_D} T}{M_\varphi^2} - 4\pi^2 \frac{(\mu_{\psi_D} + \mu_{\psi_B} - 4\mu_{\phi_D}) T^2}{M_\varphi^3} \right], \quad (15)$$

where we have assumed that the visible and dark sectors are in thermal equilibrium. We have kept $\mu_{\phi_D} \neq \mu_{\psi_D}$ to differentiate between the contributions coming from final state bosons and fermions. The logarithm of m_{ϕ_D}/T is a remnant of Bose enhancement encoded by the stimulated emission factor $(1 + f_{\phi_D})$ in Eq. 8. It arises because the phase space density diverges as $E_{\phi_D} \rightarrow \mu_{\phi_D}$ indicating that ϕ_D is condensing; the divergence is regulated by the mass m_{ϕ_D} . In the left panel of Fig. 1 we compare the analytic expression in Eq. 15 to the numerical evaluation in the limit of small chemical potentials, finding excellent agreement in the relevant range of parameters.

As expected, we see that the leading order corrections from Bose enhancement and Pauli exclusion are of the same sign. This sign is readily understood: for $\mu_{\psi_D}, \mu_{\phi_D} > 0$ (corresponding to more DM than anti-DM), Pauli exclusion

² In the other limit where final state masses are larger than the temperature, the resulting asymmetries are Boltzmann suppressed.

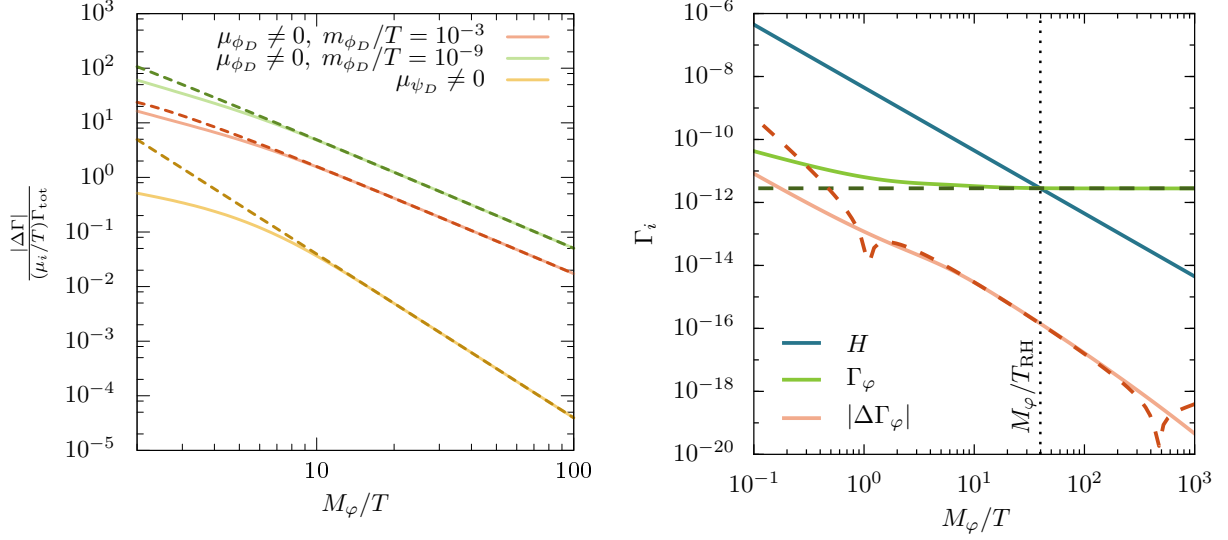


FIG. 1: Decay widths as function of M_φ/T . The left plot compares numerical computations (solid lines) to the analytic approximations (dashed lines) of the decay asymmetry discussed in the text for fixed value of m_{ϕ_D}/T . Contributions from Bose enhancement due to ϕ_D and Pauli blocking due to ψ_D are isolated by choosing $\mu_{\phi_D} \neq 0$ and $\mu_{\psi_D} \neq 0$ one at a time. The chemical potentials are assumed to be small, such that the resulting $\Delta\Gamma$ is linear in μ_i/T . The right plot compares the various physical rates to Hubble for fixed masses $m_{\phi_D} = m_{\psi_D} = m_{\psi_B} = 300$ GeV, $M_\varphi = 100$ TeV and $\Delta n_{\phi_D}/s = 10^{-5}$. As before, the solid lines are numerical calculations while the dashed lines correspond to analytic approximations. The dips in $\Delta\Gamma$ show where these approximations break down, namely where $M_\varphi/T \sim 1$ and $m_{\phi_D}/T \sim 1$.

blocks the channel with ψ_D in the final state, while Bose enhancement favors the channel involving ϕ_D . Comparing this with the definition of the asymmetry, Eq. 14, means that $\Delta\Gamma < 0$ for $\mu_i > 0$, in agreement with Eq. 15. Note that the sub-leading correction for Bose enhancement is in fact larger than the leading order effect from Pauli exclusion for $\mu_{\psi_D} = \mu_{\phi_D}$. Therefore, for the rest of the section we will focus on the dominant Bose enhancement effect.

The final important feature of Eq. 15 is that the decay asymmetry is largest at early times and higher T . As we show below, this causes the bulk of the visible sector asymmetry to be generated *well before* the majority of φ decays at $t \sim \Gamma_\varphi^{-1}$.

The system of Boltzmann equations for φ , n_{ψ_B} (Eqs. 12 and 13, respectively) and the DM is closed once we include the Friedmann equation

$$H^2 = \frac{8\pi}{3M_{\text{Pl}}^2} (\rho_R + \rho_\varphi), \quad (16)$$

and radiation (or entropy) production due to φ decays

$$\dot{\rho}_R + 4H\rho_R = +\Gamma_\varphi\rho_\varphi, \quad (17)$$

where $\rho_\varphi = M_\varphi n_\varphi$. The size of the radiation density at the time of the φ decay determines two distinct possibilities. When $\rho_\varphi \gg \rho_R$, the universe is initially φ -dominated and a large asymmetry produced by the decays is diluted by the significant entropy dump. In the opposite regime $\rho_\varphi \ll \rho_R$, the universe is radiation dominated. The above system is easily solved numerically for any choice of parameters. Sample solutions are shown in Fig. 2 for the φ - and radiation-dominated cases. Below we use approximate analytic solutions to better understand these results.

Using the same approximations as before, $\mu/T \ll m_{\phi_D}/T \ll T/M_\varphi \ll 1$, we can easily estimate the baryon asymmetry yield. This limit allows us to neglect washout reactions generated by the first term in Eq. 4, e.g. $\psi_B\psi_D\phi_D^\dagger \leftrightarrow \psi_B^\dagger\psi_D^\dagger\phi_D$, since these are suppressed by $(T/M_\varphi)^4 \ll 1$. For the analytic results below we make the additional assumption that $\mu_{\phi_D} = \mu_{\psi_D}$, i.e. that the transfer reactions $\phi_D\phi_D \leftrightarrow \psi_D\psi_D$ are in equilibrium. This ensures that $\Delta n_{\phi_D} a^3$ and $\Delta n_{\psi_D} a^3$ are constant. Note that these comoving number densities are insensitive to dilution from entropy release.

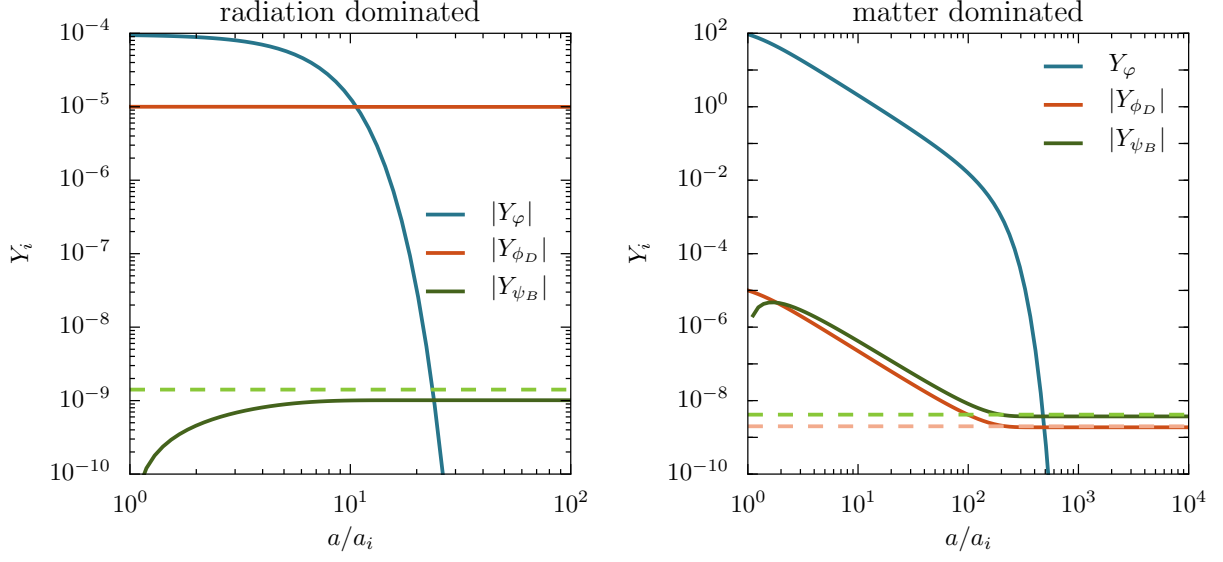


FIG. 2: Evolution of the baryon and dark matter asymmetries during φ decay for radiation-dominated (left plot) and matter-dominated (right plot) initial conditions. We chose $\rho_{\varphi,i}/\rho_{R,i} = 10^{-3}$ in the former case, and $\rho_{\varphi,i}/\rho_{R,i} = 10^3$ in the latter. The solid lines show the numerical solution of the Boltzmann equations, while the dashed lines show the analytic approximations for the final abundances discussed in the text. Note that the bulk of the visible asymmetry Y_{ψ_B} is produced before φ decays. We used $M_\varphi = 100$ TeV, $T_{\text{RH}} = 2.5$ TeV, $Y_{\phi_D,i} = 10^{-5}$ and $T_i = 3T_{\text{RH}}$ in these examples.

We first consider the radiation-dominated (RD) scenario where $\rho_\varphi \ll \rho_R \sim T^4$ prior to the decay. In this limit, the entropy produced by φ is negligible, which means that $Y_{\phi_D} \equiv \Delta n_{\phi_D}/s$ is constant. As alluded to above, one can see that the standard intuition of the asymmetry being generated by the decay occurring when $\Gamma \sim H$ is incorrect. Comparing $\Delta\Gamma$ to the Hubble rate during radiation domination $H \sim T^2/M_{\text{Pl}} \sim 1/t$:

$$\Delta\Gamma \sim \Gamma_\varphi Y_{\phi_D} \frac{T^2}{M_\varphi^2} \ln(m_{\phi_D}/T) \sim \frac{\ln t}{t}, \quad (18)$$

we find that $\Delta\Gamma/H$ is only logarithmically dependent on time and in fact favors earlier times! This means that roughly an equal amount of asymmetry is being generated every single e -folding, suggesting that the naive instantaneous decay estimate must be corrected by the number of e -foldings. This is logarithmically sensitive to the initial time, which depends on when the out-of-equilibrium φ density and the dark matter asymmetry were generated.

Using these limits, we can solve the Boltzmann equations analytically. A simple closed form can be obtained when $\Gamma_\varphi/H_i \ll 1$, where H_i is the initial Hubble rate that determines the initial time $t_i \sim H_i^{-1}$. We find the final baryon number abundance to be

$$\begin{aligned} \text{RD:} \quad \frac{Y_{\psi_B}}{Y_{\phi_D}} &= kg_* \ln \left[\frac{m_{\phi_D}^2}{2T_i^2} \right] Y_\varphi \left(\frac{T_{\text{RH}}}{M_\varphi} \right)^2 \exp \left(\frac{\Gamma_\varphi}{2H_i} \right) \left| \text{Ei} \left(-\frac{\Gamma_\varphi}{2H_i} \right) \right| \\ &\approx kg_* \ln \left[\frac{m_{\phi_D}^2}{2T_i^2} \right] Y_\varphi \left(\frac{T_{\text{RH}}}{M_\varphi} \right)^2 \log \left(\frac{\Gamma_\varphi}{2H_i} \right), \end{aligned} \quad (19)$$

where $k = 4\pi^2/5 \approx 7.9$, T_i is the initial temperature, $\text{Ei}(-z)$ is the exponential integral with $\text{Ei}(-z) \sim \gamma_E + \ln z$ for $z \ll 1$ and in the second line we used the approximation that $\Gamma_\varphi \ll H_i$. The temperature T_{RH} is defined in Eq. 20 and in the radiation-dominated regime it is used as a proxy for Γ_φ rather than an actual reheat temperature. The correct baryon number asymmetry can be obtained for reasonable values such as $Y_{\phi_D} \sim Y_\varphi \sim 10^{-4}$ and $M_\varphi \sim 10^2 T$. This analytical result is compared with the full numerical solution in the left panel of Fig. 2.

Next we consider the matter-dominated (MD) case, that is $\rho_\varphi \gg \rho_R \sim T^4$ just before the decay. In this case, φ decays generate a large amount of entropy, reheating the universe. The reheat temperature defined by $\Gamma_\varphi = H(T_{\text{RH}})$

is [24]

$$T_{\text{RH}} = \left(\frac{90}{\pi^2 g_*(T_{\text{RH}})} \right)^{1/4} \sqrt{\Gamma_\varphi M_{\text{Pl}}}. \quad (20)$$

As before, we can see that the asymmetry is produced at early times by comparing $\Delta\Gamma$ to Hubble $H \sim 1/t$:

$$\Delta\Gamma \sim \Gamma_\varphi Y_{\phi_D} \frac{T^2}{M_\varphi^2} \ln(m_{\phi_D}/T) \sim \frac{\ln t}{\sqrt{t}}, \quad (21)$$

where we have used $T \sim 1/t^{1/4}$ [25]. From this, we see that $\Delta\Gamma/H$ is largest for $t < \Gamma_\varphi^{-1}$, so most of the asymmetry is in fact generated before φ decay. The later decays are a subdominant contribution to the asymmetry.

The Boltzmann equations can be solved for $t \ll \Gamma_\varphi^{-1}$ for Δn_{ψ_B} [25, 26]. The final baryon yield $Y_{\psi_B} = \Delta n_{\psi_B}/s_f$ can then be evaluated as

$$\text{MD: } \frac{Y_{\psi_B}}{Y_{\phi_D}} \approx kg_* \ln \left[\frac{m_{\phi_D}^2}{2T_i^2} \right] \left(\frac{T_{\text{RH}}}{M_\varphi} \right)^3 \left(\frac{H_i}{\Gamma_\varphi} \right)^{3/4}, \quad (22)$$

where we assumed that the logarithmic part of $\Delta\Gamma$ is constant. The left hand side contains quantities evaluated at late times; in particular Y_{ϕ_D} includes dilution due to φ decays. The constant k is given by

$$k \approx 4 \frac{45}{2} \left(\frac{\pi^2}{30} \right) \left(\frac{2}{5} \right)^{3/4} \frac{2\Gamma(\frac{9}{20})\Gamma(\frac{3}{4})}{\Gamma(\frac{1}{5})} \approx 15.6. \quad (23)$$

Equation 22 contains the initial Hubble, indicating that it is a UV dominated process. Parametrically $Y_{\psi_B} \lesssim Y_{\phi_D}$ because the last two factors on the right hand side of Eq. 22 can be written as $(T_{\text{max}}/M_\varphi)^3$, where T_{max} is the maximum temperature achieved during reheating [25]. We require that $T_{\text{max}} < M_\varphi$ to avoid washout and to ensure that our approximations for $\Delta\Gamma$ are valid. However, the baryon asymmetry can be *larger* than the DM asymmetry even if $T_{\text{max}} \lesssim M_\varphi$ since $kg_* \sim \mathcal{O}(10^3)$ is large for T_{RH} high enough. This is demonstrated by the numerical solution of the Boltzmann equations shown in the right panel of Fig. 2. For the benchmark point shown, $T_{\text{max}}/M_\varphi \lesssim 10^{-1}$ and wash-out is expected to be unimportant. In Fig. 3 we show the baryon yield relative to the DM asymmetry for a range of initial φ densities interpolating between the RD and MD cases discussed above. The analytic solutions presented in Eqs. 19 and 22 agree well with the full numerical solution in their regions of validity away from $\rho_{\varphi,i}/\rho_R(T_i) \approx 1$.

The above results should be compared with the standard out-of-equilibrium decay scenario where $\Delta\Gamma$ does not depend on temperature and the yield $Y_{\psi_B} \approx \Delta\Gamma T_{\text{RH}}/(\Gamma_\varphi M_\varphi)$ is independent of initial conditions [27]. In the case considered in this section, a larger initial φ density (larger H_i) results in the production of a larger asymmetry. Thus we find that when Bose enhancement is responsible for communicating the asymmetry between the dark and visible sectors, initial conditions become important. In the following section we reach a similar conclusion for the class of models where Pauli blocking rather than Bose enhancement is responsible for asymmetry production.

III. ASYMMETRIES THROUGH PAULI BLOCKING

In the previous section we presented a model where a particle asymmetry was generated dominantly by Bose enhancement. In this section we consider the complementary case where the leading effect is due to Pauli exclusion. This is easily implemented in the toy theory

$$\mathcal{L} = \frac{1}{2} \varphi \bar{\psi}_B (a + ib\gamma_5) \psi_B^C + \lambda \bar{\psi}_B^C \psi_D \Phi_{DB} + \text{h.c.} \quad (24)$$

where ψ_B (and its charge conjugate ψ_B^C) and ψ_D are now Dirac fermions with masses m_{ψ_B} , m_{ψ_D} , charged under baryon and dark matter number, respectively; Φ_{DB} is a complex scalar with mass $m_{\Phi_{DB}}$, carrying opposite charge under both symmetries. Thus, the second term preserves both $U(1)_B$ and $U(1)_D$. We will show that decays of the φ will violate CP in the presence of a ψ_D asymmetry, even if they are CP -symmetric at zero temperature. As in the previous section, we assume that a ψ_B asymmetry can be converted into visible baryons, via, e.g. the neutron portal, Eq. 5.

The decays of φ tend to wash out any existing ψ_B asymmetry. For example, if there are more ψ_B than $\bar{\psi}_B$ then Pauli blocking biases φ decays to generate more $\bar{\psi}_B$, eventually destroying any baryon number present. We first

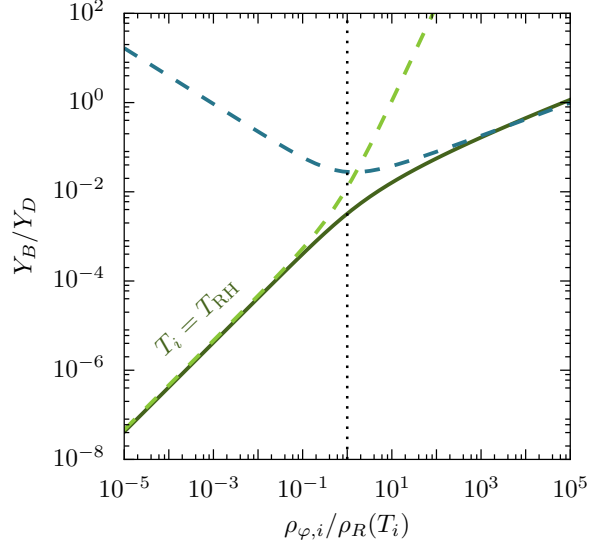


FIG. 3: Ratio of baryon to DM asymmetry yield at late times as a function of the initial φ density. The left (right) dashed lines show the approximate analytic solutions in the radiation-dominated (matter-dominated) universe as discussed in the text. We see that these analytic solutions very quickly become good approximations in their respective regions of validity.

consider what happens when there is a non-zero dark matter asymmetry and zero initial baryon number asymmetry. Conservation of $U(1)_B$ charge ensures that

$$(n_{\psi_B} - n_{\bar{\psi}_B}) - (n_{\Phi_{DB}} - n_{\Phi_{DB}^\dagger}) = 0, \quad (25)$$

which implies $\mu_{\psi_B} = \mu_{\Phi_{DB}}$ at temperatures above ψ_B and Φ_{DB} masses. The second interaction in Eq. 24 enforces chemical equilibrium

$$\mu_{\psi_B} + \mu_{\psi_D} + \mu_{\Phi_{DB}} = 0. \quad (26)$$

It is easy to solve for chemical potentials in the limit of small asymmetries, see e.g. [28]; the result is

$$Y_{\Phi_{DB}} = Y_{\psi_B} = -\frac{Y_{\psi_D}}{2}, \quad (27)$$

where $Y_i = (n_i - n_{\bar{i}})/s$. Despite the absence of any initial baryon number, ψ_B has a non-zero asymmetry.

Next we consider what happens when φ decays. As discussed above Pauli exclusion pushes the system towards a configuration where $Y_{\psi_B} = 0$. As long as there is a large enough number density of φ , Y_{ψ_B} will be driven to zero. We can now calculate the baryon number generated by the decays to find that

$$Y_B \equiv Y_{\psi_B} - Y_{\Phi_{DB}} = \frac{Y_{\psi_D} - Y_{\Phi_{DB}}}{2} = \frac{Y_D}{2} \quad (28)$$

Chemical equilibrium “hides” baryon number in the scalar states Φ_{DB} , protecting it from wash-out via φ decays. For $m_{\Phi_{DB}} > m_{\psi_B} + m_{\psi_D}$, after Φ_{DB} freezes out and decays, its asymmetry will be transferred back into ψ_B and ψ_D . Thus we see that the Pauli exclusion principle can make an otherwise CP preserving decay generate baryon number.

Note that this setup is closely related to models where baryon number is generated in thermal equilibrium [29, 30]. In particular, in Ref. [30] an existing DM asymmetry is used to bias electroweak sphalerons (which are in equilibrium prior to the electroweak phase transition) to generate a baryon asymmetry. A similar scenario is realized in the present model if $M_\varphi \lesssim T$ and the relevant couplings are large enough, such that B -violating scattering like $\psi_B \psi_B \leftrightarrow \bar{\psi}_B \bar{\psi}_B$ is in equilibrium. In this limit one can solve for the chemical potentials to find the same result of a non-zero baryon number existing in thermal equilibrium with the value shown in Eq. 28. If B -violating φ -mediated scattering continues after Φ_{DB} freeze-out and decay, any existing baryon number would be washed out, so such processes must go out of equilibrium. In Ref. [30] baryon number violating sphalerons are turned off by a first order electroweak phase transition. In our model, such a rapid shut off is not possible. Thus, we focus on the out-of-equilibrium decay scenario, where baryon number violation turns off once φ decays.

An important restriction on this model arises from the fact that the rate at which baryon number is generated is Boltzmann suppressed in the limit $M_\varphi \gg T$. This is because in the two-body decay $\varphi \rightarrow \psi_B \psi_B$, the ψ_B final state energy is fixed to be $M_\varphi/2$, while Pauli exclusion is most effective at energies below the temperature. However, in the limit where $M_\varphi \ll T$, the inverse decays $\psi_B \psi_B \rightarrow \varphi$ become important and wash out the asymmetry. Thus there is only a finite range of parameters with $M_\varphi \gtrsim T_{\text{RH}}$ where Pauli blocked decays generate a significant asymmetry. Due to the lack of parametric control, we explore this situation numerically and provide a useful analytic estimate of the final asymmetry. In the following two subsections, we first write down the coupled set of Boltzmann equations and then discuss their solutions.

A. Boltzmann Equations

The Boltzmann equations for the particle asymmetries $\Delta n_i = n_i - n_{\bar{i}}$ have the form

$$\frac{d\Delta n_i}{dt} + 3H\Delta n_i = C_i[\Delta n_j], \quad (29)$$

where C_i are the collision terms which include the effects of number-changing interactions that enforce chemical equilibrium. In writing this system of equations we approximated the phase space distributions by their Maxwell-Boltzmann limits. For simplicity we make the additional assumption of *kinetic* equilibrium and small asymmetries, i.e. $\mu_i/T \ll 1$, such that $n_i + n_{\bar{i}} \approx 2n_i^{\text{eq}}$. Note that this requires the existence of efficient interactions of the ψ_D , ψ_B and Φ_{DB} states with the thermal bath, which we leave unspecified.

Given the interactions in Eq. 24, the ψ_D and Φ_{DB} collision terms at leading order in the coupling λ include only $1 \leftrightarrow 2$ processes:

$$C_{\psi_D} = -\langle \Gamma_D \rangle \left(\Delta n_{\psi_D} + \frac{n_{\psi_D}^{\text{eq}}}{n_{\psi_B}^{\text{eq}}} \Delta n_{\psi_B} + \frac{n_{\psi_D}^{\text{eq}}}{n_{\Phi_{DB}}^{\text{eq}}} \Delta n_{\Phi_{DB}} \right) + \text{perms.}, \quad (30)$$

$$C_{\Phi_{DB}} = -\langle \Gamma_{DB} \rangle \left(\Delta n_{\Phi_{DB}} + \frac{n_{\Phi_{DB}}^{\text{eq}}}{n_{\psi_B}^{\text{eq}}} \Delta n_{\psi_B} + \frac{n_{\Phi_{DB}}^{\text{eq}}}{n_{\psi_D}^{\text{eq}}} \Delta n_{\psi_D} \right) + \text{perms.}, \quad (31)$$

where the $\langle \Gamma_D \rangle = \Gamma_D K_1(m_{\psi_D}/T)/K_2(m_{\psi_D}/T)$ is the thermally-averaged decay rate for $\psi_D \rightarrow \Phi_{DB} \psi_B^\dagger$ and similarly for Γ_{DB} ; “perms.” stands for terms with identical structure but with D , B and DB permuted. These rates are given in Appendix A. For a given choice of masses, only one of $\Gamma_{D,B,DB}$ is non-zero. Note that with the above assumptions $\Delta n_i/(2n_i^{\text{eq}}) \approx \mu_i/T$, such that the collision terms above vanish when $\mu_{\psi_D} + \mu_{\psi_B} + \mu_{\Phi_{DB}} = 0$, i.e. in chemical equilibrium.

The ψ_B collision term includes additional contributions from B -violating φ decays and φ mediated scattering. The decay contribution is given by

$$\begin{aligned} C_{\psi_B} &\supset \int d\Phi_3 |\mathcal{M}(\varphi \rightarrow \psi_B \psi_B)|^2 [f_\varphi(1 - f_{\psi_B,1})(1 - f_{\psi_B,2}) - f_{\psi_B,1}f_{\psi_B,2}(1 + f_\varphi) - (\psi_B \rightarrow \bar{\psi}_B)] \\ &\approx -\frac{1}{2M_\varphi} \int d\Phi_2 |\mathcal{M}(\varphi \rightarrow \psi_B \psi_B)|^2 \left[2n_\varphi \frac{\Delta n_{\psi_B}}{n_{\psi_B}^{\text{eq}}} e^{-M_\varphi/2T} + n_\varphi^{\text{eq}} \frac{(n_{\psi_B}^2 - n_{\bar{\psi}_B}^2)}{(n_{\psi_B}^{\text{eq}})^2} \right] \\ &= -2\Gamma_\varphi \left(\frac{\Delta n_{\psi_B}}{n_{\psi_B}^{\text{eq}}} \right) [n_\varphi e^{-M_\varphi/2T} + n_\varphi^{\text{eq}}], \end{aligned} \quad (32)$$

where in the first step we approximated $E_\varphi \approx M_\varphi$, used detailed balance to replace $f_{\psi_B,1}f_{\psi_B,2}$ by $\exp(-E_\varphi/T)n_{\psi_B}^2/(n_{\psi_B}^{\text{eq}})^2$ and performed the integral over p_φ . The former approximation (along with the Maxwell-Boltzmann limit used throughout this section) breaks down when $T \sim M_\varphi$. This is also the regime where the DM-induced decay asymmetry is largest. Note that in the last line Γ_φ is the total decay rate (both to $\psi_B \psi_B$ and $\bar{\psi}_B \bar{\psi}_B$), including a symmetry factor for identical final state particles. The full collision term can now be written as

$$\begin{aligned} C_{\psi_B} &= -\langle \Gamma_B \rangle \left(\Delta n_{\psi_B} + \frac{n_{\psi_B}^{\text{eq}}}{n_{\psi_D}^{\text{eq}}} \Delta n_{\psi_D} + \frac{n_{\psi_B}^{\text{eq}}}{n_{\Phi_{DB}}^{\text{eq}}} \Delta n_{\Phi_{DB}} \right) + \text{perms.} \\ &\quad - 2\Gamma_\varphi \left(\frac{\Delta n_{\psi_B}}{n_{\psi_B}^{\text{eq}}} \right) (n_\varphi e^{-M_\varphi/2T} + n_\varphi^{\text{eq}}) - 4\langle \sigma v \rangle_{\text{RISS}} n_{\psi_B}^{\text{eq}} \Delta n_{\psi_B}, \end{aligned} \quad (33)$$

where $\langle\sigma v\rangle_{\text{RISS}}$ is the Real Intermediate State-subtracted (RISS) wash out cross-section for the φ -mediated process $\psi_B\psi_B \leftrightarrow \psi_B\psi_B$ discussed in Appendix A 2. Using the same approximations we can write the φ collision term as:

$$C_\varphi = -\Gamma_\varphi \left(n_\varphi \left[1 - 2e^{-M_\varphi/(2T)} \right] - n_\varphi^{\text{eq}} \right). \quad (34)$$

The remaining Boltzmann equation governs the radiation density

$$\dot{\rho}_R + 4H\rho_R = -M_\varphi C_\varphi, \quad (35)$$

where the minus on the right-hand side simply cancels the one in Eq. 34. In the following section we study this system of Boltzmann equations analytically and numerically.

B. Solutions and Numerical Examples

Simple approximations to the Boltzmann equations discussed in the previous section allow us to determine the final baryon asymmetry analytically. For concreteness we assume that the universe is radiation dominated with an out-of-equilibrium φ density.³ The φ equation can be integrated neglecting inverse processes and statistical factors in the collision term of Eq. 34.⁴ Inserting the resulting solution into the Eq. 33, assuming chemical potentials are small and integrating this equation we find the baryon asymmetry

$$Y_{\psi_B} = \frac{\Delta n_{\psi_B}}{s} \approx -4 \left(\frac{\mu_{\psi_B,i}}{T_i} \right) \left(\frac{\Gamma_\varphi}{H_i} \right) [Y_{\varphi,i} f_1(M_\varphi/T_i, \Gamma_\varphi/H_i) + Y_{\varphi,i}^{\text{eq}} f_2(M_\varphi/T_i)] \quad (36)$$

where quantities with the subscript i are evaluated at the initial time and temperature. In particular $\mu_{\psi_B,i}/T_i$ can be determined from the DM asymmetry using the charge neutrality and chemical equilibrium conditions, Eqs. 25 and 26, respectively:

$$\frac{\mu_{\psi_B,i}}{T_i} = -\frac{\mu_{\psi_D,i}}{T_i} \begin{cases} 1/2 & T_i \gg m \\ (1 + n_{\psi_B}^{\text{eq}}/n_{\Phi_{DB}}^{\text{eq}})^{-1} & T_i < m. \end{cases} \quad (37)$$

Finally, the functions f_1 and f_2 have the following form in the limit $z = M_\varphi/T_i \gg 1$ and $\gamma = \Gamma_\varphi/H_i \ll 1$:

$$f_1(z, \gamma) \sim 2z^{-4} (2z^2 + z^3 - \gamma [24 + 12z + 2z^2] + \mathcal{O}(z\gamma^2)) e^{-z/2}, \quad (38)$$

$$f_2(z) \sim z^{-1} + \frac{5}{2}z^{-2} + \frac{15}{4}z^{-3} + \mathcal{O}(z^{-4}). \quad (39)$$

Note that $Y_{\varphi,i}^{\text{eq}} \sim z^{3/2} \exp(-z)$ so that both terms in Eq. 36 are Boltzmann suppressed in the non-relativistic limit. As in the Bose case considered in Sec. II, we see that the asymmetry production favors early times and higher temperatures. In fact, the bulk of the asymmetry is produced before $t \sim \Gamma_\varphi$. Note that this only holds up to $T_i \sim M_\varphi$ where the asymmetry would be damped by the (neglected) wash-out terms.

The sensitivity of the final asymmetry to early times emphasizes the importance of initial conditions in this scenario. In particular, a physical set of initial conditions depends on the origins of the φ density and DM asymmetry. There are several ways to obtain an out-of-equilibrium density of φ . The simplest mechanism for this is freeze-out, which would occur at $T \sim M_\varphi/20$. Thus the decay and asymmetry production would happen at even lower temperatures. From the analytical solution, Eq. 36, it is clear that the final asymmetry would be exponentially suppressed.

Another possibility for generating an out-of-equilibrium density of φ is the misalignment mechanism. If φ was displaced from the minimum of its potential during inflation, then its field value would remain Hubble damped until $H \sim M_\varphi$ (corresponding to a temperature $T_{\text{osc}} \sim \sqrt{M_\varphi M_{\text{Pl}}}$). At this point φ begins coherent oscillations, with the energy density in these fluctuations red-shifting as matter. The asymmetry generation cannot begin until the DM develops a chemical potential, since it is required to bias φ decays. Thus, in principle, the ψ_B asymmetry can be created any time between T_{osc} and $T_{\text{RH}} \sim \sqrt{\Gamma_\varphi M_{\text{Pl}}}$. However, as discussed above, we are working in the Maxwell-Boltzmann limit, so our Boltzmann equations are valid only for $T < M_\varphi$. Thus we confine our attention to the region

³ In a φ dominated universe φ decays deposit a large amount of entropy, diluting the newly-created baryon asymmetry. Such an entropy release can be compensated for with a higher initial DM asymmetry.

⁴ The omission of the small chemical potentials in this step corresponds to dropping sub-leading $\mathcal{O}(\mu/T)$ terms in the final asymmetry.

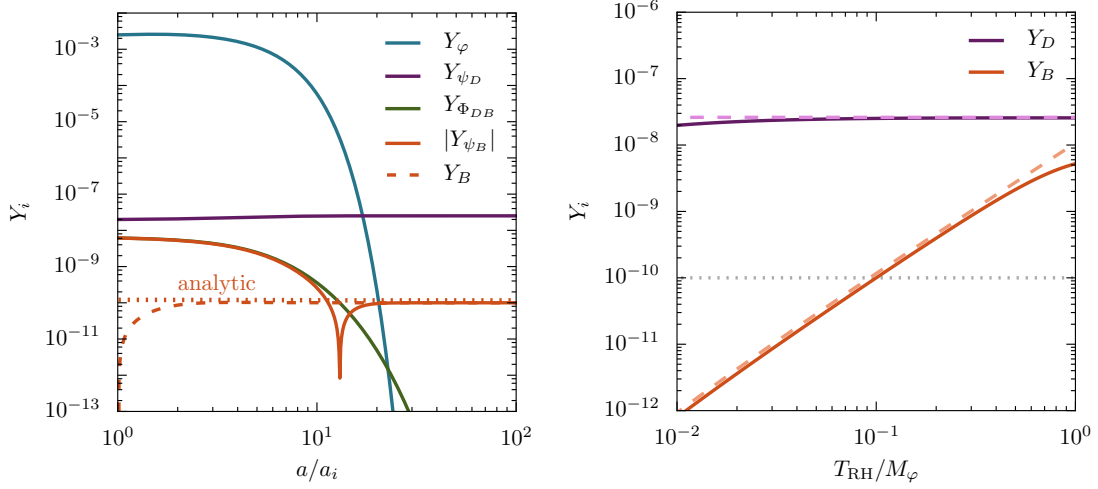


FIG. 4: Numerical solutions to the Boltzmann equations describing asymmetry production through Pauli-blocked decays of φ . The left panel shows the evolution of the various number densities as a function of the scale factor. The dotted line is the analytic approximation of Eq. 36. The dashed line shows that the net baryon number, $Y_B = Y_{\psi_B} - Y_{\Phi_{DB}}$ is produced at early times, before φ decays. The right panel shows the dependence of the final baryon yield on the decay temperature of φ , T_{RH} . The red dashed line is the analytic solution for Y_{ψ_B} , while the purple dashed line is the initial DM asymmetry. This initial asymmetry is diluted by the φ entropy injection at low T_{RH} . The initial conditions and parameter values used are described in the text.

of parameters where $T_{RH} < M_\varphi \ll T_{osc}$. We emphasize that this is not a fundamental requirement, but merely a computational aid. The condition $T_{RH} < M_\varphi$ has the additional benefit of making the rates for wash out processes, i.e., inverse decays and B -violating $2 \rightarrow 2$ scattering, very slow.

We show the numerical solutions to the system of Boltzmann equations in Fig. 4 for $M_\varphi = 1$ TeV, $T_{RH} = 100$ GeV, $T_i = M_\varphi/3$ and $\rho_\varphi(T_i) = 10^{-2}\rho_R(T_i)$. The initial DM asymmetry is chosen to be $Y_{\psi_D}/s = 2 \times 10^{-8}$ in order to obtain $Y_B = 10^{-10}$ at late times; the other asymmetries are determined from the initial $U(1)_B$ charge neutrality and chemical equilibrium requirements in Eqs. 25 and 26, respectively. The remaining masses are chosen to satisfy $M_\varphi > 2m_{\psi_B}$ and $m_{\Phi_{DB}} > m_{\psi_D} + m_{\psi_B}$: $m_{\psi_B} = 100$ GeV, $m_{\psi_D} = 150$ GeV and $m_{\Phi_{DB}} = 300$ GeV. Note, however, that the mechanism is not sensitive to a particular choice of masses, as long as the relevant processes are kinematically allowed. These initial conditions are chosen to produce the correct order of magnitude for the baryon asymmetry.

In the left panel of Fig. 4 we show the evolution of various number densities as a function of the scale factor a , normalized to a_i , its value at the initial time. At early times, chemical equilibrium with the asymmetric DM results in non-zero asymmetries for ψ_B and Φ_{DB} , while $Y_{\Phi_{DB}} = Y_{\psi_B}$ is guaranteed due to vanishing initial $U(1)_B$ charge. However, φ decays quickly drive the Y_{ψ_B} asymmetry to 0, such that the only remaining B number is stored in Φ_{DB} . When Φ_{DB} decays, its asymmetry flows into ψ_B and ψ_D , resulting in a final non-zero B number. The dashed line in this figure shows the net B number density, i.e. $Y_{\psi_B} - Y_{\Phi_{DB}}$, which explicitly shows that the B asymmetry is generated well before φ fully decays. The dotted line shows the analytic solution of Eq. 36.

In the right panel of Fig. 4 we show the final DM and baryon asymmetries as a function of T_{RH} . The light red dashed line shows the analytic solution, while the dashed purple line shows the initial DM asymmetry. Increasing T_{RH} corresponds to higher decay rates Γ_φ , which in turn, leads to more φ decaying at early times, thereby enhancing the effect of Pauli blocking and asymmetry generation. Note that this cannot continue indefinitely, because at a high enough temperature wash out due to inverse decays and $2 \leftrightarrow 2$ reactions becomes important. We do not extend the calculation to $T_{RH}/M_\varphi > 1$ because the Maxwell-Boltzmann approximation used throughout this section breaks down, but as emphasized before, this is not a fundamental limitation of this scenario. Note that at low T_{RH} the entropy injection due to φ decays is large enough to partially dilute the initial DM asymmetry, resulting in a decreased Y_D yield.

IV. DISCUSSION AND CONCLUSION

In this paper we have investigated CP violation through matter effects at finite temperature in the early universe. We have shown that quantum statistical effects play a crucial role in this class of baryogenesis models. We considered models where the visible sector Lagrangian is CP invariant and CP violation arises from an asymmetric background density of particles. Such a background is expected to exist, if, e.g., dark matter is asymmetric or if there is another quasi-stable asymmetric species during this epoch. Out-of-equilibrium baryon number violating decays of a scalar φ were shown to generate baryon number in this background, despite the absence of CP violation in the interactions of φ . This is distinct from the standard out-of-equilibrium decay scenario employed in, e.g., leptogenesis or GUT baryogenesis, where CP is violated through the interference of tree and loop contributions to the decay rate. Instead, the dark matter asymmetry biases φ decay to prefer some channels over others through Pauli blocking or Bose enhancement of the corresponding final states. We considered two toy models where only one of these effects is dominant. Thus, we provide the first example of a baryogenesis scenario where statistical factors play a critical role – no asymmetry is produced when Pauli blocking and Bose enhancement are neglected.

Finally, we note that the models considered in this paper are far from complete. While they illustrate the general “ CP violation through matter effects” mechanism, we have not attempted to embed them in realistic scenarios, which, e.g., describe the φ production mechanism in the early universe, the origin of baryon number violation, or the nature of the dark sector asymmetry. These details are important for setting the initial conditions which play a crucial role in determining the baryon yield when the B -violating decay asymmetry is generated by quantum statistical effects. Moreover, these directions may identify concrete experimental probes for this class of models. A complete model of baryon number violation in our scenarios (i.e. a UV completion of the non-renormalizable operators in Eqs. 4 and 5) may be testable at nucleon decay or neutron oscillation experiments. Similarly, different mechanisms of generating the dark matter asymmetry can give rise to observable signatures. For example, if the dark asymmetry is created in a strongly first order phase transition à la electroweak baryogenesis, a detectable gravitational wave background may be generated. The necessity for interactions between the dark and visible sectors in our scenarios suggests the possibility of complementary probes. We leave a detailed investigation of these issues to future work.

ACKNOWLEDGMENTS

We thank Brian Shuve and Falko Dulat for useful conversations and Yanou Cui for stimulating discussions that led to this work. N.B. is supported by DOE Contract DE-AC02-76SF00515. A.H. is supported by the DOE Grant de-sc0012012 and NSF Grant 1316699.

Appendix A: Wash-out and Decay Rates in the Pauli Scenario

In this Appendix we collect the decay rates and wash-out cross-section relevant for the scenario in discussed in Sec. III.

1. Decays

The first term in Eq. 24 gives rise to B -violating φ decays with the rate

$$\Gamma(\varphi \rightarrow \psi_B \psi_B) = \Gamma(\varphi \rightarrow \bar{\psi}_B \bar{\psi}_B) = \frac{M_\varphi}{32\pi} [|a|^2 + |b|^2 - 4y^2|a|^2] [1 - 4y^2]^{1/2}, \quad (\text{A1})$$

where $y = m_{\psi_B}/M_\varphi$. Assuming these are the only two channels the total φ decay rate is

$$\Gamma_\varphi = \frac{M_\varphi}{16\pi} [|a|^2 + |b|^2 - 4y^2|a|^2] [1 - 4y^2]^{1/2}. \quad (\text{A2})$$

The second term in Eq. 24 is responsible for sharing the $U(1)_B$ and $U(1)_D$ numbers, such that φ decays generate

a baryon asymmetry. The leading physical processes that enforce this are the following decays and inverse decays

$$\Gamma_{DB} = \Gamma(\Phi_{DB} \rightarrow \bar{\psi}_D \bar{\psi}_B) = \Gamma(\Phi_{DB}^\dagger \rightarrow \psi_D \psi_B) = \frac{|\lambda|^2}{8\pi} m_{\Phi_{DB}} \beta(m_{\Phi_{DB}}, m_{\psi_D}, m_{\psi_B}), \quad (\text{A3})$$

$$\Gamma_B = \Gamma(\psi_B \rightarrow \bar{\psi}_D \Phi_{DB}^\dagger) = \Gamma(\bar{\psi}_B \rightarrow \psi_D \Phi_{DB}) = \frac{|\lambda|^2}{16\pi} m_{\psi_B} \beta(m_{\psi_B}, m_{\psi_D}, m_{\Phi_{DB}}), \quad (\text{A4})$$

$$\Gamma_D = \Gamma(\psi_D \rightarrow \Phi_{DB}^\dagger \bar{\psi}_B) = \Gamma(\bar{\psi}_D \rightarrow \Phi_{DB} \psi_B) = \frac{|\lambda|^2}{16\pi} m_{\psi_D} \beta(m_{\psi_D}, m_{\Phi_{DB}}, m_{\psi_B}), \quad (\text{A5})$$

where

$$\beta(x, y, z) = \frac{|m_{\Phi_{DB}}^2 - (m_{\psi_B} + m_{\psi_D})^2|}{x^2} \left[1 - \frac{(y+z)^2}{x^2} \right]^{1/2} \left[1 - \frac{(y-z)^2}{x^2} \right]^{1/2} \theta(x - y - z). \quad (\text{A6})$$

Note that for a given mass ordering only one of these rates is non-zero.

2. Scattering and Real Intermediate States

In addition to φ decays, the B -violating interaction in Eq. 24 induces the wash-out reaction $\psi_B \psi_B \leftrightarrow \bar{\psi}_B \bar{\psi}_B$ with an intermediate s -channel φ . If this process is active it will drive any existing baryon asymmetry to zero. Fortunately, the rate for this wash out process is small when φ decays out-of-equilibrium, as required in the scenario of Sec. III. However, this rate can be enhanced when the intermediate φ goes on-shell, so we evaluate it below. The corresponding cross-section is

$$\sigma v_{\text{lab}} = \frac{1}{128\pi s} \frac{(1 - 4m_{\psi_B}^2/s)^{1/2}}{(1 - 2m_{\psi_B}^2/s)(1 - M_\varphi^2/s)^2} \left(|a|^2 + |b|^2 - \frac{4m_{\psi_B}^2}{s} |a|^2 \right)^2 \quad (\text{A7})$$

$$\approx \frac{|b|^4 m_{\psi_B}^2}{16\pi M_\varphi^4 (1 - 4m_{\psi_B}^2/M_\varphi^2)^2} \sqrt{\epsilon} + \mathcal{O}(\epsilon^{3/2}), \quad (\text{A8})$$

where $\epsilon = (s - 4m_{\psi_B}^2)/4m_{\psi_B}^2$ is the kinetic energy per unit mass in the lab frame [31, 32]. Note that the leading contribution from the scalar interaction $\propto a$ is velocity suppressed. This is because the bilinear $\bar{\psi}_B \psi_B^C$ can only create states with orbital angular momentum $L = 1$ [33]. The thermal average can be performed analytically in the large $x = m_{\psi_B}/T$ limit or numerically, keeping all ϵ and x dependence in the cross-section. The analytical result is

$$\langle \sigma v \rangle (\psi_B \psi_B \leftrightarrow \bar{\psi}_B \bar{\psi}_B) = \frac{1}{\sqrt{\pi x}} \left(\frac{|b|^4 m_{\psi_B}^2}{16\pi M_\varphi^4 (1 - 4m_{\psi_B}^2/M_\varphi^2)^2} \right), \quad (\text{A9})$$

where the quantity in the braces is the cross-section at threshold. We are interested in this rate while ψ_B and $\bar{\psi}_B$ are still in chemical equilibrium, which means x is not large. Moreover, for long-lived φ the cross-section is strongly peaked around the resonance, away from $\epsilon = 0$. This means that the ϵ expansion is not valid. The full rate (without making these approximations) is then determined by numerically performing the integral⁵

$$\langle \sigma v \rangle (\psi_B \psi_B \leftrightarrow \bar{\psi}_B \bar{\psi}_B) = \frac{x}{K_2(x)^2} \int d\epsilon \sqrt{\epsilon} (1 + 2\epsilon) K_1(2x\sqrt{1+\epsilon}) \sigma v_{\text{lab}}, \quad (\text{A10})$$

where we included a factor of 1/2 for identical initial states in the definition of the thermal average. This rate includes processes occurring through on-shell φ exchange when $s = M_\varphi^2$. However, the on-shell decays and inverse decays $\varphi \leftrightarrow \psi_B \psi_B$, $\bar{\varphi} \leftrightarrow \bar{\psi}_B \bar{\psi}_B$ are already present in the Boltzmann equations – see Eq. 33. To avoid double counting the

⁵ This thermal average procedure is valid only in the non-relativistic limit, so the results for $x \lesssim 1$ should be considered to be rough estimates.

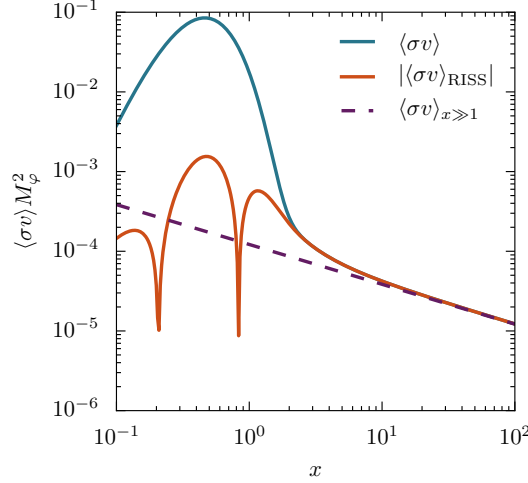


FIG. 5: Thermally averaged cross-section for $\psi_B\psi_B \leftrightarrow \bar{\psi}_B\bar{\psi}_B$ as a function of $x = m_{\psi_B}/T$ for $a = 0$, $b = 1$ and $m_{\psi_B}/M_\varphi = 0.1$. The solid blue line is the standard thermal average computed from the numerical integral in Eq. A10, which includes the resonant enhancement for $s \approx M_\varphi^2$. The solid orange line shows same cross-section with the real intermediate state contribution subtracted to avoid double counting in solving the Boltzmann equations. The dashed line is the analytical large x approximation from Eq. A9.

resonant contribution to $\langle\sigma v\rangle(\psi_B\psi_B \leftrightarrow \bar{\psi}_B\bar{\psi}_B)$ must be subtracted [34–36]. One simple approach to implement this Real Intermediate State (RIS) subtraction is to modify the squared s channel propagator as

$$\frac{1}{(s - M_\varphi^2)^2 + \Gamma_\varphi^2 M_\varphi^2} \rightarrow \frac{1}{(s - M_\varphi^2)^2 + \Gamma_\varphi^2 M_\varphi^2} - \frac{\pi}{M_\varphi \Gamma_\varphi} \delta(s - M_\varphi^2), \quad (\text{A11})$$

where Γ_φ is the total decay rate. The RIS contribution corresponding to the Dirac delta function is easily computed:

$$\langle\sigma v\rangle_{\text{RIS}} = \frac{1}{2M_\varphi^2} \frac{\pi^2 x K_1(x/y)}{y^5 K_2(x)^2} \text{Br}(\varphi \rightarrow \psi_B\psi_B) \text{Br}(\varphi \rightarrow \bar{\psi}_B\bar{\psi}_B) \frac{\Gamma_\varphi}{M_\varphi} \quad (\text{A12})$$

$$= \frac{n_\varphi^{\text{eq}}}{(n_{\psi_B}^{\text{eq}})^2} \text{Br}(\varphi \rightarrow \psi_B\psi_B) \text{Br}(\varphi \rightarrow \bar{\psi}_B\bar{\psi}_B) \frac{K_1(x/y)}{K_2(x/y)} \Gamma_\varphi. \quad (\text{A13})$$

In the last line we wrote the RIS rate in terms of the equilibrium distributions for ψ_B and φ . The proper RIS-subtracted (RISS) rate that enters the Boltzmann equation 33 is obtained by taking the difference of Eqs. A10 and A13. We compare the RIS-subtracted cross-section with other approximations in Fig. 5. Note that the RISS cross-section becomes negative in the resonance region near $x \sim 1$. Numerically this happens because the RIS rate in Eq. A13 is slightly larger than the standard rate in Eq. A10; this, in turn, is because of the finite width of the resonance peak. This was also observed in Ref. [37].

-
- [1] A. G. Cohen, A. De Rujula, and S. L. Glashow, *Astrophys. J.* **495**, 539 (1998), arXiv:astro-ph/9707087 [astro-ph].
 - [2] A. Sakharov, *Pisma Zh.Eksp.Teor.Fiz.* **5**, 32 (1967).
 - [3] V. A. Kuzmin, V. A. Rubakov, and M. E. Shaposhnikov, *Phys. Lett.* **B155**, 36 (1985).
 - [4] D. E. Morrissey and M. J. Ramsey-Musolf, *New J. Phys.* **14**, 125003 (2012), arXiv:1206.2942 [hep-ph].
 - [5] D. V. Nanopoulos and S. Weinberg, *Phys. Rev.* **D20**, 2484 (1979).
 - [6] M. Fukugita and T. Yanagida, *Phys. Lett.* **B174**, 45 (1986).
 - [7] A. Riotto, in *Proceedings, Summer School in High-energy physics and cosmology: Trieste, Italy, June 29-July 17, 1998* (1998) pp. 326–436, arXiv:hep-ph/9807454 [hep-ph].
 - [8] W. Buchmuller, R. D. Peccei, and T. Yanagida, *Ann. Rev. Nucl. Part. Sci.* **55**, 311 (2005), arXiv:hep-ph/0502169 [hep-ph].
 - [9] S. Davidson, E. Nardi, and Y. Nir, *Phys. Rept.* **466**, 105 (2008), arXiv:0802.2962 [hep-ph].
 - [10] A. D. Linde, *Phys.Lett.* **B160**, 243 (1985).
 - [11] M. P. Hertzberg and J. Karouby, *Phys.Rev.* **D89**, 063523 (2014), arXiv:1309.0010 [hep-ph].

- [12] J. Unwin, (2015), arXiv:1503.06806 [hep-th].
- [13] A. Hook, JHEP **11**, 143 (2015), arXiv:1508.05094 [hep-ph].
- [14] M. Giovannini and M. E. Shaposhnikov, Phys. Rev. **D57**, 2186 (1998), arXiv:hep-ph/9710234 [hep-ph].
- [15] M. M. Anber and E. Sabancilar, Phys. Rev. **D92**, 101501 (2015), arXiv:1507.00744 [hep-th].
- [16] T. Fujita and K. Kamada, Phys. Rev. **D93**, 083520 (2016), arXiv:1602.02109 [hep-ph].
- [17] K. Kamada and A. J. Long, (2016), arXiv:1610.03074 [hep-ph].
- [18] S. H.-S. Alexander, M. E. Peskin, and M. M. Sheikh-Jabbari, Phys.Rev.Lett. **96**, 081301 (2006), arXiv:hep-th/0403069 [hep-th].
- [19] K. M. Zurek, Phys. Rept. **537**, 91 (2014), arXiv:1308.0338 [hep-ph].
- [20] H. Davoudiasl, D. E. Morrissey, K. Sigurdson, and S. Tulin, Phys. Rev. Lett. **105**, 211304 (2010), arXiv:1008.2399 [hep-ph].
- [21] A. G. Cohen and D. B. Kaplan, Phys. Lett. **B199**, 251 (1987).
- [22] A. G. Cohen and D. B. Kaplan, Nucl. Phys. **B308**, 913 (1988).
- [23] R. T. D’Agnolo and A. Hook, Phys. Rev. **D91**, 115020 (2015), arXiv:1504.00361 [hep-ph].
- [24] T. Moroi and L. Randall, Nucl. Phys. **B570**, 455 (2000), arXiv:hep-ph/9906527 [hep-ph].
- [25] G. F. Giudice, E. W. Kolb, and A. Riotto, Phys. Rev. **D64**, 023508 (2001), arXiv:hep-ph/0005123 [hep-ph].
- [26] D. J. H. Chung, E. W. Kolb, and A. Riotto, Phys. Rev. **D60**, 063504 (1999), arXiv:hep-ph/9809453 [hep-ph].
- [27] E. W. Kolb and M. S. Turner, Front. Phys. **69**, 1 (1990).
- [28] J. A. Harvey and M. S. Turner, Phys. Rev. **D42**, 3344 (1990).
- [29] K. Blum, A. Efrati, Y. Grossman, Y. Nir, and A. Riotto, Phys. Rev. Lett. **109**, 051302 (2012), arXiv:1201.2699 [hep-ph].
- [30] G. Servant and S. Tulin, Phys. Rev. Lett. **111**, 151601 (2013), arXiv:1304.3464 [hep-ph].
- [31] P. Gondolo and G. Gelmini, Nucl.Phys. **B360**, 145 (1991).
- [32] J. Edsjo and P. Gondolo, Phys.Rev. **D56**, 1879 (1997), arXiv:hep-ph/9704361 [hep-ph].
- [33] J. Kumar and D. Marfatia, Phys. Rev. **D88**, 014035 (2013), arXiv:1305.1611 [hep-ph].
- [34] E. W. Kolb and S. Wolfram, Nucl. Phys. **B172**, 224 (1980), [Erratum: Nucl. Phys.B195,542(1982)].
- [35] G. F. Giudice, A. Notari, M. Raidal, A. Riotto, and A. Strumia, Nucl. Phys. **B685**, 89 (2004), arXiv:hep-ph/0310123 [hep-ph].
- [36] A. Pilaftsis and T. E. J. Underwood, Nucl. Phys. **B692**, 303 (2004), arXiv:hep-ph/0309342 [hep-ph].
- [37] J. M. Cline, K. Kainulainen, and K. A. Olive, Phys. Rev. **D49**, 6394 (1994), arXiv:hep-ph/9401208 [hep-ph].